2

Phase Change Materials for Solar Energy Applications

Hoda Akbari,[a] David G Peña,[a] Rebeca S Pizarro,[a] Hind Ahmed,[a] Maria C. Browne,[a] Chuka O'koli,[a] Edward Guionneau,[a] Ming Jun Huang[b] and Sarah J. McCormack[a,c,*]

[a]*Department of Civil, Structural and Environmental Engineering, Trinity College, Dublin 2, Ireland*
[b]*School of Architecture and the Built Environment, Built Environment Research Institute, Ulster University, Belfast, UK*
[c]*Dublin Energy Lab., Dublin Institute of Technology, Grangegorman, Dublin 7, Ireland*

**Corresponding author*: mccorms1@tcd.ie

2.1 Introduction

Increasing levels of greenhouse gas (GHG) emissions and energy dependency on other countries have brought governments to develop and improve various ways of producing energy. There are many different methods of renewable production of energy. Currently, solar photovoltaics are one of the most popular methods and rapidly increasing with a worldwide growth of 60% over 5 years from 2007 to 2012 [1]. This is due to fact that solar panels are simply designed products that require low maintenance and are easy to install.

Photovoltaic systems can be installed on nearly all terrain permitting easy distribution of the energy produced among a community or country assisting resolving local grid issues. Furthermore, they also allow energy independence on a local or even national scale, which is a major geopolitical issue for many countries.

Although, before 2010 the electricity produced by a PV system was much more expensive than that produced by wind and geothermal power and up to 6 times more expensive than electricity produced by coal and gas [2], presently the PV cost has decreased 4-5 times becoming a real alternative in the close future to the fossil fuels [3].

Phase Change Materials, edited by Vikas Mittal

This high cost of PV energy is due to the high cost of PV panels and their low level of efficiency - they only convert 15% to 20% of solar radiation into electricity energy.

The applications for photovoltaic (PV) systems differ and they include field, transport and building applications. Over the decade, the incorporation of photovoltaics as an integrated part of buildings has exponentially increased. They are referred to as building integrated photovoltaic systems (BIPV) and have one of the fastest growing markets globally [4]. BIPV systems possess many advantages and are summarized as follows [5]:

I. When PV systems are integrated, unified or mounted onto buildings, they mitigate against the cost of acquiring land and associated costs like fencing and cost of support structures which are required for ground installation of the PV modules.
II. The overall cabling costs can be significantly reduced because the buildings are typically connected to the grid.
III. The losses and cost that are correlated with the transmission and distribution of electricity are mitigated against, because the electricity is being originated close to the point of use.
IV. The integration of PV into buildings displace the use of other building materials while performing structural duties like weather protection.

Due to PV cells being the most expensive component of a photovoltaic system, the idea of concentrating solar radiation into a smaller area of cells gave prospect into reduction of the system overall cost [6]. The reduction in the BIPV system can be achieved either through the increase of the system efficiency or through replacement of the PV components (PV cells) with reflective material [7]. The use of the reflective or refractive material in the latter concentrates solar energy onto the PV cells allowing for an increased luminous flux on the PV cell surface [7], a reduced cell area per output and a reduced overall system cost per unit of energy produced [6].

Furthermore, the efficiency of solar cells decreases by 0.5% for every degree increase above the solar cells standard operating temperature [8]. If the trends of increasing PV electricity production are going to continue, the efficiency of PV cells need to be maintained during high temperature conditions. Phase change materials (PCMs) can absorb or release heat while they are changing phase, for instance from solid to liquid. PCMs have melting ranges at which the

temperature stays constant until the material is fully liquefied or solidified; referred to as the latent heat stage. During this stage, PCMs can absorb or release large amounts of heat energy. The phase change process results in a cooling effect which has proven to be very useful at regulating temperatures in various applications. Previous experiments undertaken combining PCMs and solar panels have shown very encouraging results [9]. However, one of the main issues that was highlighted is the material would not always fully re-solidify overnight, meaning that the PCM would not have maximum capacity for use the next day.

Most solar radiation reaching a PV cell is converted into thermal energy increasing the cell temperature. Temperature increases in photovoltaic (PV) module lead to immediate efficiency losses and can accelerate long-term degradation. Silicon PV modules operated at elevated temperatures exhibit lower efficiency in converting solar energy into electrical energy. Temperature elevation is inevitable when the rate of solar heat gained by the PV is higher than the rate of heat lost to the ambient environment [10].

2.2 Phase Change Materials

PCMs are materials that have the capacity to absorb heat while they change phase. As the phase change happens in their latent heat stage, the temperature of the material stays constant as heat gets absorbed or rejected, at that point the material is in a mix phase, a mixture of solid and liquid. Heat will be absorbed or released until the material reaches its maximum heat capacity or is fully discharged at which point the material will be fully melted. Once the material is back into a single phase, the temperature will start increasing or decreasing again. Water is a good example of a PCM. The temperature of an ice cube will quickly reach 0 °C and will stay constant at that temperature until it is completely liquefied, which is the latent heat stage. As it liquefies or solidifies, heat from the atmosphere will be absorbed by the material.

In 1978, it was suggested that PCM could act as a potential thermal storage if integrated with a PV. This concept was patented in 1983 [11], but was not developed commercially. However, following this, PCM was not investigated as a means of cooling PV until the mid 1990s.

The advantages of PCMs are (i) no volume change during phase transition; (ii) increase in specific heat transfer area (large surface to

volume ratio); (iii) no leakage of PCM from matrix; (iv) protection from external environment; (v) easy application; (vi) improvement in material compatibility; (vii) improved handling during production; (viii) improved cycling stability since phase separation is restricted to microscopic distances, etc. Hence, extent of enhancement increases with heat flux, which is also investigated further by comparing the materials in the systems designed for PV for CPC and other related thermal applications.

When undergoing phase transition, PCMs can provide temperature stabilization. They are used in one of two main ways: temperature control or thermal energy storage (TES) [12]. Due to the low thermal conductivity of PCMs, their categorical use for temperature control and energy storage is finite. The effect of solidification at the heat transfer surface can lead to a significant reduction in heat transfer when energy is extracted from the liquid phase [13]. A PCM heats reasonably at initial heating, but on getting to the melting/solidification temperature, there is absorption of the latent heat by the material which leads to phase change from a solid to a liquid or a liquid to a gas. As the PCM melts, its temperature stabilizes even as it continues to absorb heat during the phase change. The temperature range and time taken, over which the phase change occurs, depend on the mass and thermal conductivity of PCM and any enhanced heat transfer elements therein [14]. This process is illustrated by Gunther *et al*. [15]. PCM can yield compact thermal energy storage over a precise temperature range, and once PCM has fully changed phase, the material will begin to heat sensibly again.

Ideal PCMs must have a large latent heat of fusion, high thermal conductivity in both liquid and solid phase with no phase separation and a melting temperature lying in the practical range of operation. They should mostly melt congruently with minimum sub-cooling. They also should be chemically stable, non-toxic, non-flammable and non-corrosive. Besides that, they must also have low density variation and a high overall density. Of all these attributes, the most difficult to achieve is high thermal conductivity. Once all the characteristics are met, the PCM would ideally be cheap and abundant.

PCMs are divided into organic (paraffin, fatty acid), inorganic (hydrated salts) and eutectic (mixture of organic or inorganic PCM) within the required melting temperature of 20 °C to 100 °C. Cabeza *et al*. divided PCMs into groups [16]:

- Cooling applications up to 21 °C

- 22-28 °C for comfort in building applications
- 29-60 °C for hot water applications
- High temperature applications requiring PCM of between 61 °C and 120 °C.

Organic PCMs are characterized by presence of carbon atoms [17]; they usually have low melting temperatures (below 220°C) and are therefore generally used for room heating. Non-Paraffin compounds include esters, acids and alcohols. Organic PCMs have very low corrosion and good thermal/chemical stability but have low latent and thermal conductivity [18].

On the other hand, inorganic PCMs have greater latent heat but are worse with respect to corrosion than organic PCMs and also have weaker thermal stability. Salt hydrates, a type of inorganic PCM, are formed by water absorption by the anhydrous salt at ambient temperatures. They have a phase change enthalpy that depends on bond strength between water molecules and the salts [17,18]. For high temperature storage (above 420 °C), molten salts have been widely used which fall into the inorganic PCM category [18].

Siegel *et al*. [19] commenced a simplified analysis to determine the heat transfer enhancement provided by the inclusion of high conductivity particles in a low conductivity salt. It was assumed the particles inside the container retained a uniform distribution during both freezing and melting cycles, while they neglected sub-cooling energy. It was resolved that there was an increase in the thermal conductivity in both the melting and solidifying processes due to the embedded particles. It was observed that depending on the ratio of particle to matrix conductivity, the particles occupying 20% of the storage by volume increased the rate of heat extraction by 10% to 20%.

Cabeza *et al*. [20] initiated experimental tests to study the heat transfer enhancement of PCM for a small thermal energy storage device using stainless steel fins, copper fins or a graphite composite material. It was concluded that the addition of stainless steel fins in the PCM did not increase the heat flux considerably, and the addition of copper pieces enhanced heat transfer especially during the melting process. The highest heat transfer flux of the three methods was found using the graphite composite material which showed a heat transfer four times higher than that of the pure PCM. The paraffin used in this analysis was RUBITHERM RT 30 and it had a melting point of 30 °C. Comparisons of PCM melting and solidification with and without fins were made and it was observed that the heat

transfer during solidification was greater if fins were included, and a 40% reduction in the solidification time was achieved.

Experimental tests and numerical simulations were undertaken [21] to study the thermal behavior of PV/PCM systems. The numerical simulations were validated by the experimental measurements. In the experimental work, the PCM RT25 with a melting temperature of 26.6 °C was used and comparisons of three different systems was carried out, which included a single flat aluminum plate system, a PV/PCM system without internal fins and a PV/PCM system with internal fins. All systems used in the experiment had the same sized front aluminum plate which was 0.3 m long and 0.132 m high, along with a uniform applied solar intensity of 750 W/m^2 at the front surface. Observations showed that after 60 minutes, the front surface temperature of the single plate system was constant at 63 °C. The front surface of the PV/PCM system without fins retained a temperature of around 36 °C between 50 and 100 minutes, then it slowly increased to 44 °C at 280 minutes. The front surface of the PV/PCM system with two fins maintained a temperature of around 32 to 33 °C between 50 to 100 minutes, and then sharply increased to 38 °C at 170 minutes. Conclusions were made that the fins facilitated a more uniform temperature distribution within the PV/ PCM system. Simulations further determined that for a south east orientated PV/PCM system having a 30 mm depth and no fins in the PCM container, the front surface temperature could be maintained at less than 35 °C for UK weather data during the summer solstice. The simulations were repeated for three consecutive days for confirmation [21]. The authors also conducted an experimental evaluation of PCMs for PV cooling. It was determined that RUBITHERM RT25 had an improved thermal control potential than that of RUBITHERM GR40 for the PV panel. Experimental tests on embedding different numbers and types of fins in the PCM to improve the effect of thermal management of PVs were also conducted. Huang *et al*. [22] reported the development of a three-dimensional numerical model which was used to simulate a phase change material container attached to a PV system. The PCM was used to regulate the temperature rise of the PV cells. For regulation of the temperature of PV cells, a PCM possessing suitable phase transition temperature is required. With PCM, high efficiencies of the PV cells can be maintained for an extended period of time [23,24]. The advantage of PCM is its ability to not only store heat but also allow for the heat to be used asynchronously [25]. An experimental evaluation of the effects of convection and crystalline segregation in

a PCM as a function of efficiency of heat transfer within the finned PV/PCM system has been studied [26]. The thermal performances of bulk PCM with crystallization segregation for different internal fin arrangements are presented. It is noted that the addition of internal fins improves the temperature control of the PV in a PV/PCM system.

2.3 The Use of PCMs for Solar Energy Applications

The use of PCM with solar technologies has been shown to maintain the efficiency of some solar energy technologies and can also be used as an energy store which can be charged during daylight hours to be used during the night.

The availability of solar energy is limited to the central hours of the day, and there is a large variation in the intensity of solar radiation throughout the year as can be seen in Figure 2.1. Currently, there is a wide variety of technologies that harness solar energy [27]. One of the most efficient technologies is solar thermal energy systems, either through flat collectors or through complex concentration systems. In these types of installations, the objective is the heating of a fluid. In order to understand the potential applications of PCMs with

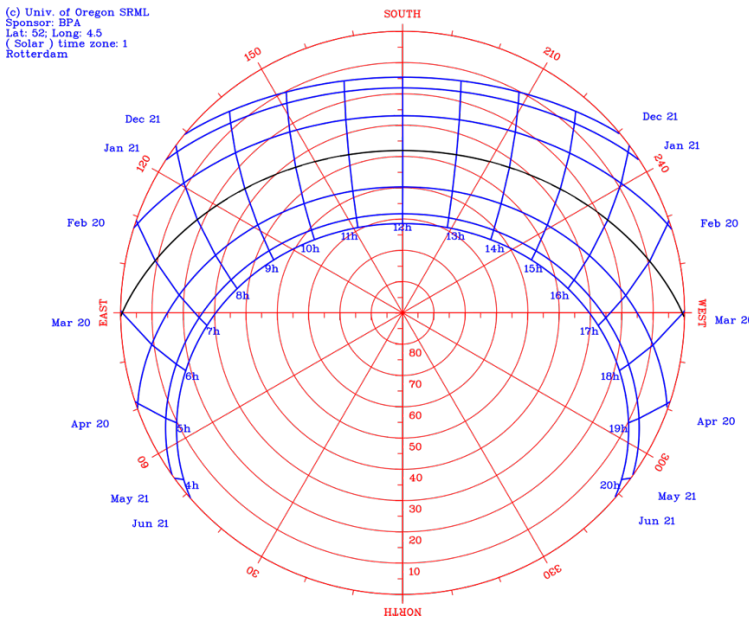

Figure 2.1 Polar diagram for Rotterdam. Sun path lines along the year.

different solar energy technologies, each of technology will be described below.

2.3.1 Solar Thermal Energy for Building and Industry

The use of low temperature solar thermal energy in homes and industries [28] is becoming increasingly widespread. These systems allow, on one hand, a saving in energy cost, as well as a reduction of CO_2 emissions as solar energy is a clean and renewable resource that can replace the use of fossil fuels. Through solar collectors, it is possible to convert solar energy into thermal energy that is transferred into a liquid or gaseous fluid that is circulated inside, usually water or air. These collectors can be divided into two categories: non-concentrating and concentrating. Domestic thermal solar energy mainly implements non-concentrating collectors that can be either flat plate or evacuated tube collectors [29]. Flat plate collectors, as shown in Figure 2.2 (left), are of simple geometry, cost efficient, robust and effective even with diffuse solar radiation. Evacuated tube collectors contain vacuum-sealed tubes with a heat pipe inside, as illustrated in Figure 2.2 (right). Convection and conduction losses are reduced by the vacuum, so it can operate at higher temperatures in comparison with flat plate collectors. Their efficiency in day-long performance is also higher at lower incidence angles due to their geometry.

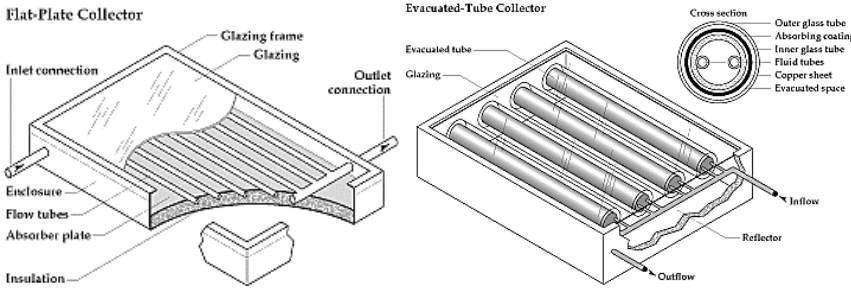

Figure 2.2 Schematic diagram of a flat plate collector (left) and evacuated tube collector (right) for solar energy (Source: U.S. Department of Energy).

However, the variability of solar radiation makes it necessary to use thermal storage systems (TES). During the central hours of the day, when solar radiation is higher, energy consumption decreases, having an excess of heat that, if it is not stored, is dissipated into the environment.

In case of having thermal energy storage (TES) systems in the installation, it is possible to use the excess energy during the peaks of energy demand or in the night. Traditionally, TES in solar thermal for domestic and industrial installations has been carried out by large tanks of fluid [30-32], usually water, where heat is stored by raising the temperature of the fluid (sensible heat). It is possible to store heat with a lower volume and greater stability of the fluid temperature through the use of PCM in these tank designs which is shown in Figure 2.3 [33-35]. These factors allow the installation costs to be lower, in addition to being able to install higher power in homes with small spaces. The wide variety of existing PCMs [31,36] allows to adjust the temperature of the phase change to the optimal operating temperature of the heating system, domestic hot water or to the industrial process.

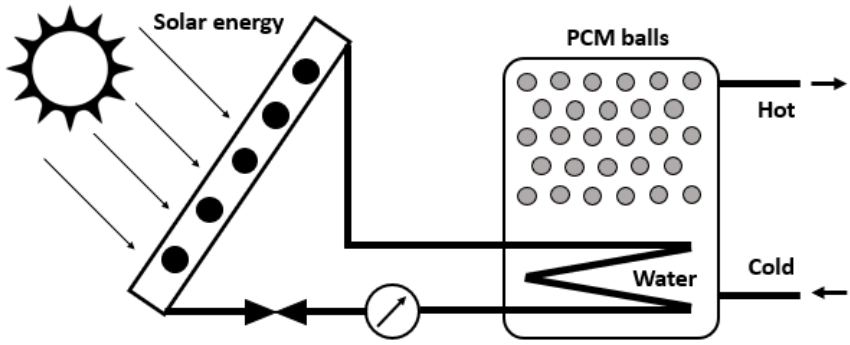

Figure 2.3 Schematic of a solar thermal installation with a TES-PCM.

The main limitation of PCMs is the low thermal conductivity of some materials. For this reason, a significant effort is being made by researchers to achieve optimized tank designs or develop new materials with higher thermal conductive properties that allow an efficient operation. The work of Kenisarin & Mahkamov [31] includes a complete review of different system design with fins or different geometries of PCM containers that improve the thermal conductivity of the system. Figure 2.4 shows an example of 4 geometries with fins, where it is verified that the most optimal geometry is represented in Figure 2.4(d) due to the higher number of fins which increase the heat transfer surface in contact with the PCM.

In the work of Sharif *et al*. [30], a detailed review of different PCM applications in domestic hot water systems is presented. In addition

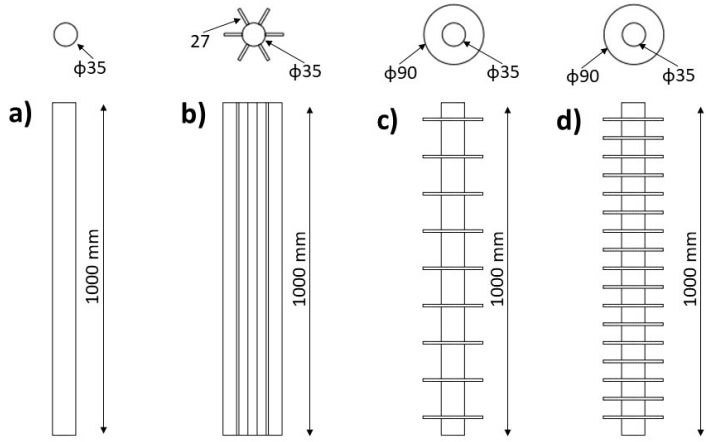

Figure 2.4 Geometries studied to increase the heat transference in a PCM system: a) single tube, b) rectangular fins, c) 17 circular fins and d) 34 circular fins.

to presenting a comparison between different tank geometries for TES with PCM, it is worth highlighting the comparisons of different solar collectors with PCM integration within the collector itself. Figure 2.5 shows four geometries analyzed in the work. The design is to stabilize the temperatures of the collector during its operation as well as to have TES integrated in the solar collector.

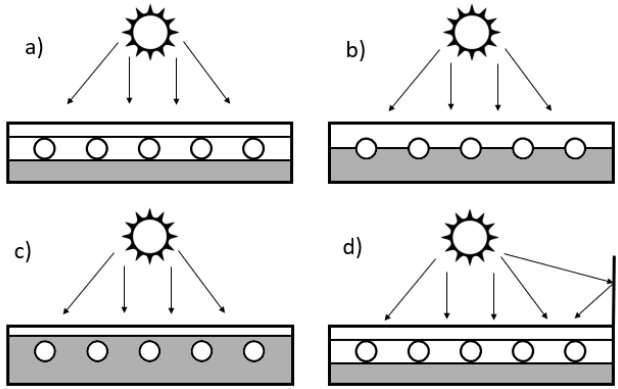

Figure 2.5 Schematic of a flat plate solar collector with PCM technologies (a) below tubes, (b) half perimeters of the tubes, (d) immersed tubes, (d) with reflector, (1) tubes, (2) absorber, (3) glass cover, (4) PCM, (5) air layer, (6) insulation and (7) reflector.

Recently low concentration systems are being developed for domestic and industrial applications. These collectors achieve higher fluid temperature. Some designs exhibit systems with PCM integration, as it can be seen in Figure 2.6. It was found the implementation of PCM in the solar collector tank extended the time for which it could supply hot water by up to 25% in 80 °C charging mode.

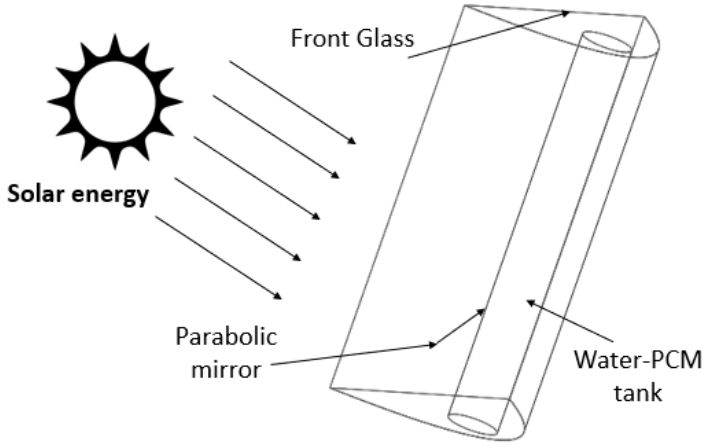

Figure 2.6 Cross-sectional schematic of the integrated collector storage solar water heater.

2.3.2 Concentrating Solar Power (CSP) Plants

Solar thermal power plants can generate large amounts of electricity through solar concentration systems that heat a fluid which is then expanded in a turbine. All these plants have parabolic mirror systems (linear or circular) which project the sun's rays onto the tube through which the fluid circulates or flat mirror systems that reflect the radiation in the focus of a tower. Unlike the low concentration systems, CSP plants have high concentration collectors, with concentrating ratios higher than 50. The higher the solar concentration is, the higher fluid temperature can be achieved and, therefore, the installation performance is improved. At present, there are four types of CPS technologies for the generation of electrical energy, which are schematically shown in Figure 2.7.

Due the high levels of concentration achieved in CSP, the temperature of the working fluid can be extremely high, over 500 °C. This

feature of CSP allows high efficiency thermodynamic cycles to being able to generate a large amount of electrical energy.

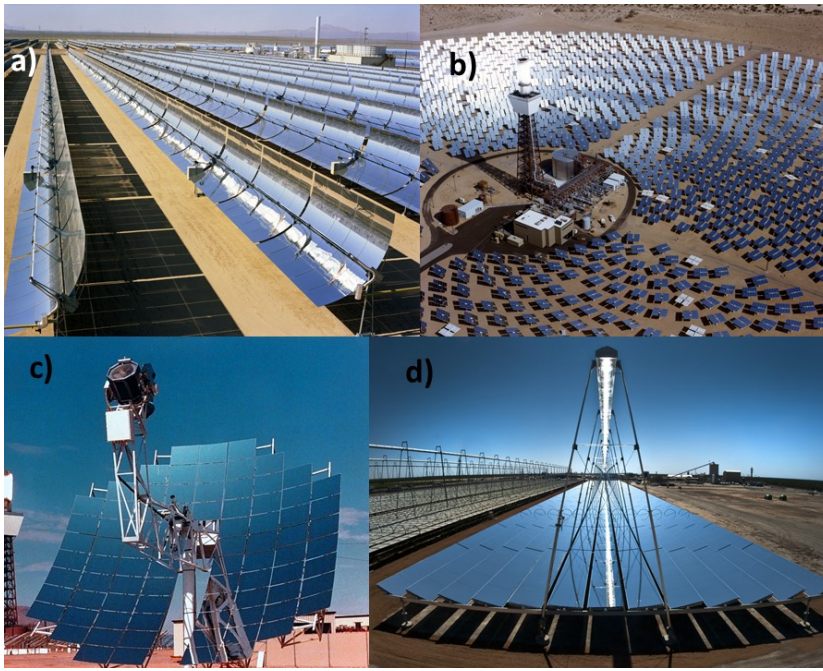

Figure 2.7 Concentrating solar power installations: a) parabolic trough system, b) solar power tower, c) parabolic dish system and d) Fresnel reflectors (Source: NREL).

Currently, Spain is the country with the most operating CSP systems [37]. With 2304 MW installed, it is almost half of the power of the operational plants in the world. New CSPs will start operating in a few years, thus, the power capacity of this technology will be doubled. The most common technology is a parabolic troughs system [38], as is cheaper, simpler and easier to optimize as compared with the other technologies.

In the design of such facilities, special care is taken with the location with a large number of hours of sunshine per year, as the solar power plants require TES to generate electrical power without interruption for greater number of hours. In some installations, auxiliary boilers are installed, that allow generating electricity in periods of insufficient radiation.

Due to the high working temperature of these facilities and a large

amount of energy that is necessary to store, the best alternative for TES is the use of PCM [39-42], with molten salts the most commonly used. Most of the operating plants currently use as PCM a mixture of 60% sodium nitrate and 40% potassium nitrate.

The installations with thermal accumulation have oversized collectors to generate an excess of energy that covers the turbine's energy demand for a period of between 4-8 hours [37,38]. This energy is stored in two large thermally insulated tanks (Figure 2.8), one cold and other hot. During daylight hours, the salts are pumped from the cold PCM tank to a heat exchanger, where the PCM increases its internal energy, and subsequently stored in the hot tank. When the solar radiation decreases or disappears, the cycle is reversed, where PCM is the medium that heats the working fluid of the installation in the exchanger to produce steam.

Figure 2.8 Salt tank for heat storage in CSP (Source: U.S. Department of Energy).

The geometry of the accumulation tanks is usually cylindrical and may contain tens of thousands of tonnes of PCM, depending on the number of hours of night operation and the power of the CSP plant. Figure 2.9 shows the outline of a complete installation of parabolic trough, where it is possible to see one of the most common distributions of heat storage tanks.

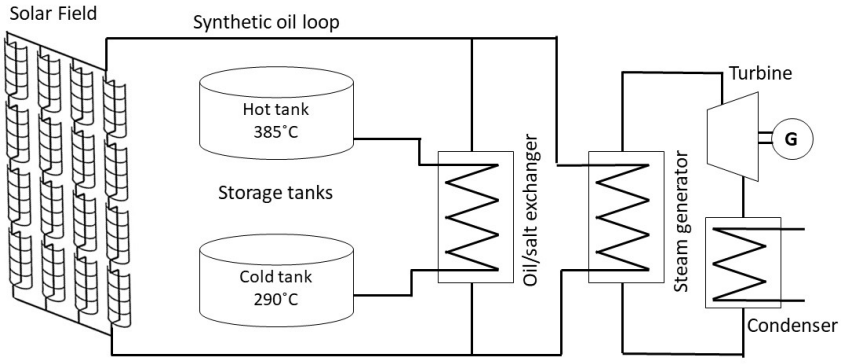

Figure 2.9 CSP installation diagram with thermal storage.

2.3.3 PCM in Photovoltaic (PV) and Hybrid Solar Energy (PV/T)

Efforts to improve the performance of solar energy are focused in two directions, improving the materials of the PV cells or cooling the PV panels. It is at this point where the PCMs are used as a tool to improve the performance of solar PV [43,44]. In order to maintain the efficiency of the PV cell, it is necessary to remove the solar energy absorbed that has not been transformed into electricity. This residual heat produces an overheating of the cells that causes a reduction in the efficiency of 0.4-0.65 %/K [45]. During operation, a PV panel can reach temperatures up to 80 °C. It is, therefore, necessary to keep the solar panel temperature as low as possible to increase the efficiency of the installation.

Adhering a volume of PCM on the back of the PV panel, it is possible to control the temperature of the panel [44]. PCM absorbs the residual heat in the form of latent heat, thus, stabilizing the panel temperature. Three of the first design concepts were tested and compared by Huang *et al*. [21,24]. The authors compared aluminum plate to simulate a PV cell, aluminum plate with a container filled with PCM to simulate a PV/PCM system and an aluminum plate with a container filled with PCM and integrated fins. Integrated PCM system with fins demonstrated effective temperature regulation of the plate. A schematic of the system tested by Huang *et al*. is presented in Figure 2.10, where temperatures below 34 °C were obtained. For optimal system operation, the PCM to be implemented in these cases must have a melting point between 25-40 °C and due to the low thermal

conductivity of these materials, it is not recommended to work with thicknesses greater than 30 mm.

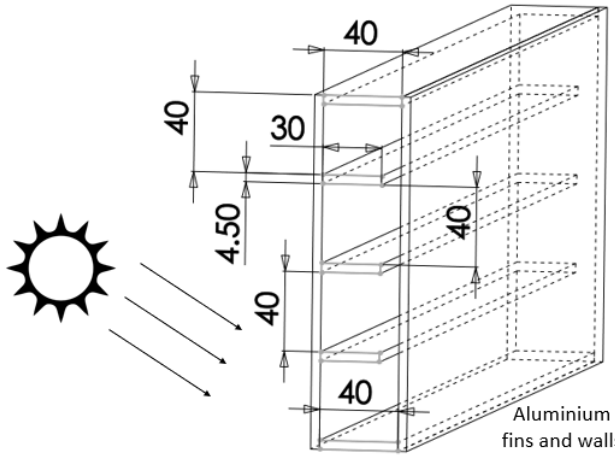

Figure 2.10 Outline and performance graph of PV panel with PCM.

The effects of convection and crystalline segregation in a PCM as a function of efficiency of heat transfer within the PV/PCM system has been experimentally investigated by Huang *et al*. [26]. The thermal performances of bulk PCM with crystallization segregation for different internal fin arrangements are presented. It is noted that the addition of internal fins improves the temperature control of the PV in a PV/PCM system. Two PCMs with different phase transient temperatures for improving the heat regulation have been predicted (see Figure 2.11) [26].

Hasan *et al*. [9] used five different PCM types (RT20, capric: palmitic acid, capric: lauric acid, calcium chloride and SP22) to enhance the thermal regulation of PV. Four different systems were tested under different insolation values (500 W/m^2, 750 W/m^2 and 1000 W/m^2) in a small-scale indoor experiment using a solar simulator. For insolation levels of 500 W/m^2, system A with capric: lauric and capric: palmitic was shown to maintain a lower PV temperature for the longest period (up to 2.5 hours at 10 °C lower than the reference system). At 750 W/m^2 and 1000 W/m^2, system A with calcium chloride was shown to maintain PV front surface temperatures 10 °C below the reference for a prolonged period of time compared to the other systems.

Also, a full-scale outdoor experiment was undertaken in Dublin,

Ireland and Vehara, Pakistan [9]. The PV panels were identical with 65 W capacity. One of the modules was used in the experiment as a reference and the other two were PV-PCM systems with eutectic mixture of capric-palmitic and salt hydrate. The results were compared at peak instantaneous temperature of the reference PV. Capric: palmitic PV-PCM system regulated the PV by 7 °C and the PV-PCM system with salt hydrate maintained a temperature reduction of 10 °C compared to the reference PV. Although in the PV-PCM configuration, the amount of electric power is higher compared to a standard PV panel, the heat absorbed by the PCM is not used. For this reason, hybrid PV/Thermal (PV/T) solar energy system was developed which converts solar radiation into electrical and thermal energy [25].

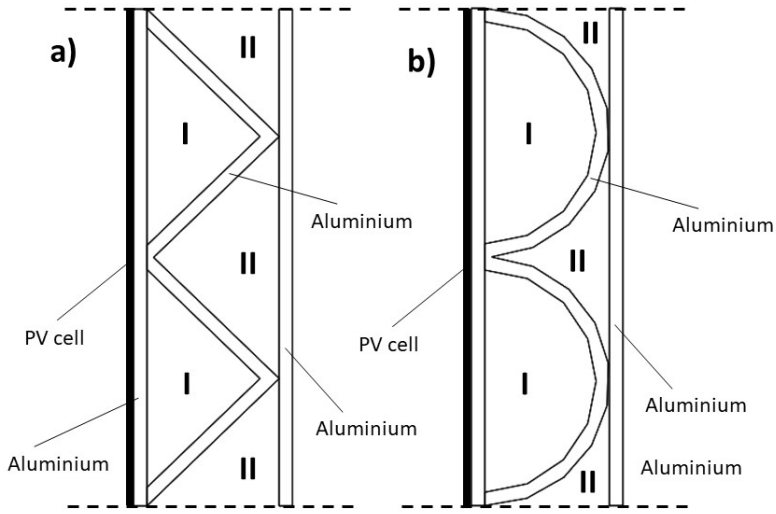

Figure 2.11 Schematic diagram of PV/PCM system with metal cells for different PCMs.

A PV/T (photovoltaic and thermal panel) system using phase change materials was designed and installed in Dublin to analyze its behavior and performance, as presented in Figure 2.12. The system was made from a standard PV panel which was disposed on a steel container full of PCM and equipped with piping network in the PCM. The aim of the set-up was to use the PCM to absorb the heat during the day and, therefore, make the PV panel more efficient by cooling it down and subsequently release the heat to the water piping in the evening and at night as the ambient temperature drops. Thus, the

water going through the piping network would be heated at a more convenient time, such as when users come back home from work. This system was compared to three reference systems: a standard solar panel, a standard equipped with a steel container on the back of it and a PV equipped with a steel container and piping network inside the container (PV/T). Four used 80 W monocrystalline silicon solar panels were used in the experiment. The container was made from steel as it has a high thermal conductivity (16 W/m K) as well as a high resistance to corrosion which can be an issue while using phase change materials. ThePCM used for the PV/T/PCM system was capric: palmitic mixture (25% capric and 75% palmitic) which has a phase change between 16 and 25 °C.

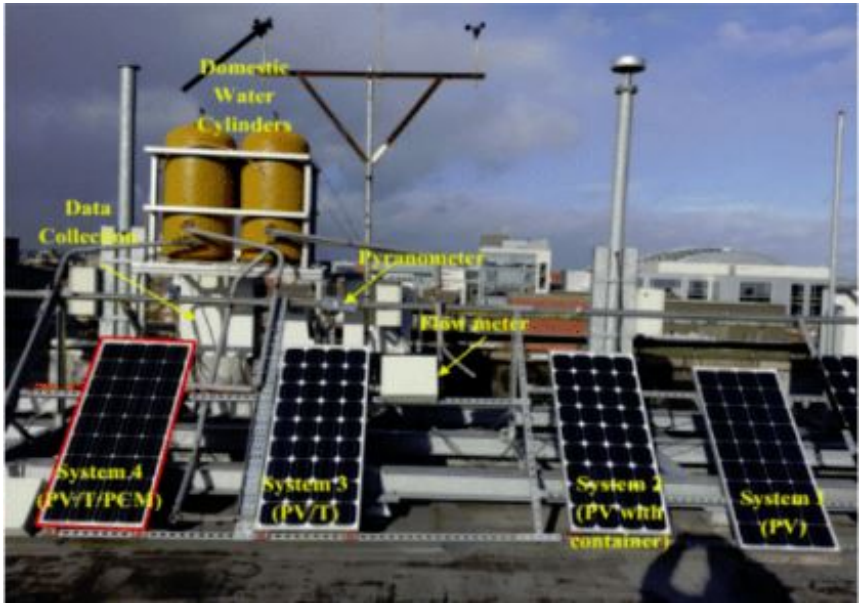

Figure 2.12 Experimental set-up of PV-PCM systems, location of thermocouples and attachment of PV to PCM container. Adapted from Reference 25 with permission from Elsevier.

Adding the PCM improved the performance of PV/T system as water was heated at a higher temperature during a longer period. The maximum water temperature difference between the PV/T and PV/T/PCM reached 5.5 °C at 6:00 am. PV/T/PCM also showed to be more efficient than the other systems on the electrical side as the

temperature of the system was regulated by PCM, thus, the panel was cooled down. The PCM improved the heat extraction up to seven times compared to the system without it [46].

Several review papers have been published on the use of PCM as a thermal management technique of PV, emphasizing the growing body of literature in the area [14,43,47,48]. Yin *et al*. [49] presented a PV/T system with integrated heat storage. Figure 2.13 presents a schematic design of different configurations of PV/T collectors for either air (right) or water (left).

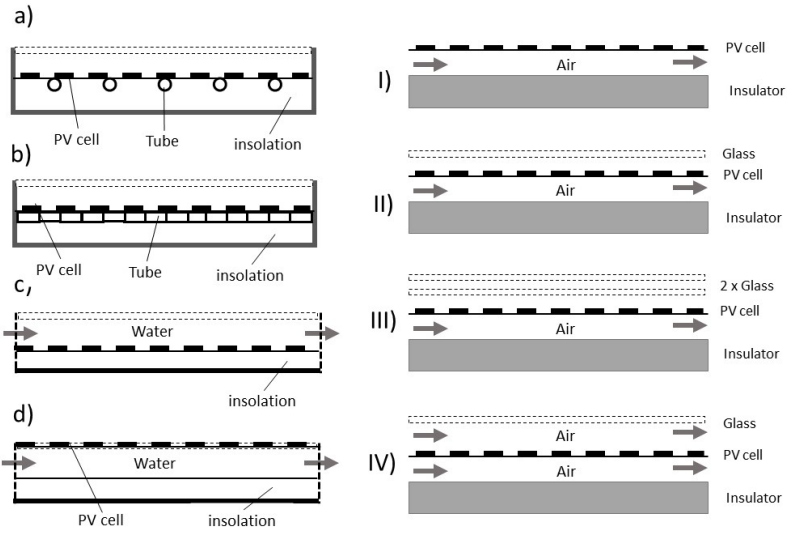

Figure 2.13 Diagram of collectors PV/T water (left) and air (right) [47].

The use of PCM in PV/T installations is in the heat accumulation tanks, just as in the case of conventional thermal solar panels. Several review papers have been published on the use of PCM as a thermal management technique of PV [14,43,49].

Subsequently, PV/T panels are being developed with modules that integrate a volume of PCM in the same PV/T panel. In this way, as in the PV-PCM, the temperature of the cells remains stable, in addition to the heat being stored in the PV/T panel itself. Figure 2.14 presents the design scheme proposed by Malvi *et al*. [50] for distribution of the PCM in the PV/T. The optimum thickness of PCM was found to be 30 mm which increases the PV efficiency by approximately 6.5%. The electrical output of the PV/T/PCM system was shown to increase by 9% when compared to a PV system only.

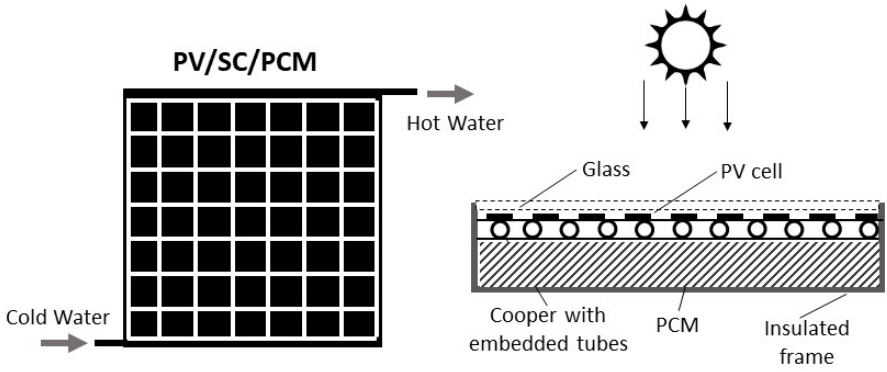

Figure 2.14 Schematic of a PV/T-PCM system.

Although it is possible to find numerous designs of systems in the literature to increase the efficiency of PV panels with PCM, most are not commercially exploited. The extra cost of including PV panel heat absorption systems and the complexity of some designs make it difficult for these technologies to be viable at present. It is only possible to find commercialized PV/T water systems [51] without integrating PCM.

2.4 Corrosion

Corrosion is a natural process which involves the deterioration of a material due the environment. In the case of the PCM in solar applications, it is critically important to study the corrosion between the PCM and the container material used for PCM encapsulation. As mentioned before, the most used PCMs in this field of applications are organic and salt inorganic PCMs, the corrosion behavior in each case is different.

2.4.1 Inorganic Compounds

Inorganic compounds are highly corrosive, for this reason it is necessary to perform the corrosion tests over different temperature ranges to ensure the container materials are compatible with their PCM. The most common inorganic PCM are the salts and salt hydrates. The most common salt hydrates for these applications are summarized in Table 2.1. This section also presents the compatibility of the salt hydrates with various materials.

Table 2.1 Summary of corrosion affects from inorganics PCMs

PCM	Mel. Pt. (°C)	Heat of fusion (kJ/kg)	Recommendations					Ref.
			Copper	Brass	Alumi-num	Stain less	Steel	
$ZnCl_2 \cdot 3H_2O$	10	---	Do not use	---	Do not use	Use	Do not use	52
$K_2HPO_4 \cdot 6H_2O$	13	---	Caution	---	Do not use	Use	Do not use	52
$NaOH \cdot 1.5H_2O$	15	---	Do not use	---	Do not use	Use	Caution	52
SP21E	21	160	Use	---	Caution	Use	Caution	53
$CaCl_2 \cdot 6H_2O$	36	170.5	Use	Use	Use	Use	Caution	54, 55, 61
TH29	29		Use	Use	Do not use	Cau-tion	Do not use	56
$Na_2SO_4 \cdot 10H_2O$	32	248	---	---	---	---	---	57
$Na_2HPO_4 \cdot 12H_2O$	35	280	Caution	Use	Do not use	Use	Caution	54, 55
$Zn(NO_3)_2 \cdot 6H_2O$	36	149.6	Do not use	Do not use	Do not use	Use	Do not use	54, 55
$Ca(NO_3)_2 \cdot 4H_2O$	42.7	---	Caution	---	---	---	Caution	58, 59
$K_3PO_4 \cdot 7H_2O$	45	---	Do not use	---	Do not use	Use	Use	52
$Zn(NO_3)_2 \cdot 4H_2O$	36	---	Do not use	---	Do not use	Do not use	Do not use	52
$Na_2S_2O_3 \cdot 5H_2O$	48	220	Do not use	Do not use	Caution	Use	Caution	56
$MgSO_4 \cdot 7H_2O$	48.5	202	Do not use	---	---	Use	Do not use	52
$NaOAc \cdot 3H_2O$	58	---	Caution	Caution	Use	Use	Use	56
$Mg(NO_3)_2 \cdot 6H_2O$	88.9	163	Caution	---	---	---	Caution	58, 59
$MgCl_2 \cdot 6H_2O$	114.5	135	Do not use	---	Do not use	Do not use	---	60

Zinc Chloride Trihydrate ($ZnCl_2 \cdot 3H_2O$)

Moreno *et al*. [52] carried out an exhaustive study of the behavior of the salt hydrated with different metals. Copper and stainless steel

found non-significant corrosion after 12 weeks, where at four weeks there was a corrosion rate of 4.4 mg/cm^{2}yr and at 12 weeks 1.7 mg/cm^{2}yr in the case of copper, however, the corrosion rate was negligible in the case of stainless steel. Carbon steel was highly corroded after 12 weeks, also a decrease of the corrosion rate with time was detected. Aluminum was the most affected with aggressive corrosion after 1 week.

Potassium Hydrogen Phosphate Hexahydrate ($K_2HPO_4 \cdot 6H_2O$)

This salt hydrate was studied by Moreno *et al*. [52] with copper and stainless steel. The authors found non-significant corrosion, however, a high corrosion rate at the beginning was detected with carbon steel and aluminum, however, after 4 weeks, the corrosion rate decreased. It continued to decrease in the case of carbon steel after 12 weeks, but increased again with aluminum.

Sodium Hydroxide Hydrated ($NaOH \cdot 1.5H_2O$)

The behavior of $NaOH \cdot 1.5H_2O$ with copper showed some corrosion, but the sample did not present any change. With stainless steel, the corrosion was observed to be negligible. Carbon steel initially had a high corrosion rate than after four and twelve weeks. Very aggressive behavior was observed with aluminum [52].

Calcium Chloride Hexahydrate ($CaCl_2 \cdot 6H_2O$)

Ren *et al*. [61] studied the behavior of the salt hydrated with two types of aluminum, carbon steel and copper at different temperatures (30, 50 and 80 °C). The authors found that the corrosion of copper increased with temperature and time, where the solution became blue at 50 °C due the corrosive products and a vivid blue solution was detected at 80 °C. Moreover, no pitting corrosion was detected. In the case of carbon steel, the mass loss increased with time and the corrosion rate decreased. The authors detected an oxide layer on the sample that could act as a protection layer. Also, the solution was transparent-yellow and dark precipitates were found at 50 and 80 °C, along with no detection of pitting corrosion. In aluminum 5086, the mass loss increased and the corrosion rate decreased with time due to the formation of a protective oxide layer. At 30 °C, there was no pitting corrosion detected. However, at 50 °C and 80 °C, minimal

pitting areas was found. Aluminum 6061 presented small pitting areas at 30 and 50 °C after 14 weeks, but pitting corrosion appeared at 80 °C after four weeks and increased with time.

Cabeza *et al*. [54,55] found that aluminum immersed in this salt was covered with a non-continuous layer after three days. After two weeks, the solution pH changed from 6 to 7/8 as a consequence of the $Al(OH)_3$ products in the solution. After 72 days, the sample was partly covered with a black layer. Copper, brass and stainless steel presented no change in the solution or in the sample and the results of mass loss and corrosion rate were negligible. However, the solution became yellow with steel and the sample was covered with a black layer after three days. The solution was bright yellow with brown precipitates after two weeks. The mass loss increased after two weeks and the corrosion rate decreased with time.

Sodium Sulfate Decahydrate ($Na_2SO_4 \cdot 10H_2O$), Glaubers Salt

García-Romero *et al*. [57] studied the behavior of this salt in contact with different aluminum types. The test was carried out with samples partly and fully immersed in the PCM. The 2024 and 1050 alloy showed increased corrosion after 30 days, but mass loss was negligible when partly immersed. However, fully immersed material remained non-corroded, which confirmed the corrosion mechanism observed in the aerated specimens, due to different oxygen concentration in different zones. In the case of 3003 and 6063 alloys, no sign of corrosion and no loss of brightness in any case (full or partly immersed) were observed.

Sodium Hydrogen Phosphate Dodecahydrate ($Na_2HPO_4 \cdot 12H_2O$)

Cabeza *et al*. [54,55] found the aluminum in contact with this salt hydrate presented significant extent of white precipitate ($Al(OH)_3$) after three days with a mass loss of 35 mg. The corrosion rate was high after three days and subsequently decreased with time. In contact with brass, copper and stainless steel, no change in the samples was observed and the corrosion results were statistically insignificant.

Zinc Nitrate Hexahydrate ($Zn(NO_3)_2 \cdot 6H_2O$)

Cabeza *et al*. [54,55] studied this PCM in short and medium term and in contact with five different materials: aluminum, brass, copper,

stainless steel and steel. In the case of aluminum, the mass loss increased with the time, but no increase of mass loss was detected after two weeks. The sample presented a layer of white precipitate and the solution had the same precipitate, which was due to the presence of hydroxide of aluminum ($Al(OH)_3$). The formation of this layer led to a decrease of the corrosion rate. After 75 days, the samples were highly corroded and the presence of the white precipitate increased. The behavior with brass was different, the solution became blue and brown precipitates were detected. The mass loss increased with time and the corrosion rate decreased, however, was higher than the aluminum samples. With copper, a blue solution and brown precipitates were also seen. The sample was fully covered by a grey layer after three days, which became black after one week. The mass loss at three days and one week was the same as brass, which did not increase subsequently, while the corrosion rate was higher after three days, followed by a decrease. After 75 days, the sample was severed with a marked increase in mass loss, and the solution became yellow with blue precipitate. Stainless steel did not show any change, but the solution became yellow as a product of the dissolution of iron ions (Fe^{3+}). The mass loss and the corrosion rate were negligible. After 75 days, the sample showed nearly no corrosion, however, brown precipitate was visible. In the case of steel, brown precipitate was detected after three days, which increased with time. The weight loss was significant, and the corrosion rate was the highest.

Calcium Nitrate Tetrahydrate ($Ca(NO_3)_2{\cdot}4H_2O$)

The compatibility of this salt was studied with carbon steel. After 700 hours, mass loss and an insoluble layer of 30 μm were observed, followed by the detection of cracks in the layer [59]. With copper, a non-compact layer of Cu_2O with precipitation products of $Cu_2(NO_3)(OH)_3$ were observed. Up until 300 hours, mass loss was detected, however, the formation of a layer was observed afterwards [58].

Tripotassium Phosphate Heptahydrate ($K_3PO_4{\cdot}7H_2O$)

The corrosion behavior of this salt hydrate with copper was initially higher, but still had lower values after four and twelve weeks in contrast with aluminum which underwent aggressive corrosion under same conditions. Stainless steel and carbon steel showed very low rates of corrosion [52].

Zinc Nitrate Tetrahydrate ($Zn(NO_3)_2{\cdot}4H_2O$)

Zinc nitrate tetrahydrate showed very high corrosion rate in contact with copper (1 week 1167 mg/cm^{2}yr, 4 weeks 644 mg/cm^{2}yr and 12 weeks 338.5 mg/cm^{2}yr), carbon steel (1 week 1741 mg/cm^{2}yr, 4 weeks 484.4 mg/cm^{2}yr and 12 weeks 196.2 mg/cm^{2}yr) and aluminum (1 week 181.5 mg/cm^{2}yr, 4 weeks 206.2 mg/cm^{2}yr and 12 weeks 162.2 mg/cm^{2}yr). However, the corrosion rate was negligible with stainless steel [52].

Sodium Thiosulfate Pentahydrate ($Na_2S_2O_3{\cdot}5H_2O$)

Moreno *et al*. [52] studied the behavior of this salt with common materials. Copper showed a very high corrosion rate after one week with a maximum of 2663.5 mg/cm^{2}yr, which subsequently decreased to 437 mg/cm^{2}yr and remained constant until 12 weeks. Carbon steel and aluminum had a similar result, a value of 40 mg/cm^{2}yr after 1 week, 15 mg/cm^{2}yr after 4 weeks and at 5 mg/cm^{2}yr after 12 weeks. Stainless steel did not show any signs of corrosion and the results were negligible.

Cabeza *et al*. [56] found that aluminum and stainless steel were corrosion resistant with this salt hydrate. However, brass and copper had a significant mass loss and both had a black precipitate after few days. Steel was seen to have corrosion with insignificant mass loss, but black precipitate appeared after 70 days.

Magnesium Sulfate Heptahydrate ($MgSO_4{\cdot}7H_2O$)

This salt hydrate showed a corrosive behavior initially in contact with copper with a value of 121 mg/cm^{2}yr, but dropped to 43 mg/cm^{2}yr after four weeks. After twelve weeks, it dropped again to 21 mg/cm^{2}yr. In contact with carbon steel, a very high value of 749.8 mg/cm^{2}yr after one week was observed, which decreased to 277.4 mg/cm^{2}yr at four weeks and ended with a value of 80.5 mg/cm^{2}yr at twelve weeks. In contrast, aluminum and stainless steel had low corrosion rates [52].

Sodium Acetate Trihydrate ($NaOAc{\cdot}3H_2O$)

The effect of sodium acetate trihydrate with common materials was studied by Cabeza et al. [56]. The authors detected that aluminum,

steel and stainless steel did not present corrosion and the solution did not exhibit any change. In the case of brass and copper, mild corrosion was detected after 70 days.

Magnesium Nitrate Hexahydrate ($Mg(NO_3)_2 \cdot 6H_2O$)

In the case of carbon steel, it was found to have a weight decrease during the first 500 hours. Afterwards, a constant corrosion rate of 11.9 mg/cm^{2}yr was maintained. Copper exhibited a different reaction, where an increased mass loss was found at the beginning due to the formation of oxide layer (Cu_2O) and oxide products of $Cu_2(NO_3)(OH)_2$, with a corrosion rate of 8.6 mg/cm^{2}yr [58]. With aluminum, during the first 500 hours of the test, the mass loss was constant and subsequently increased markedly with a corrosion rate of 2.9 mg/cm^{2}yr [54].

2.4.2 Organic Compounds

Organic compounds are recommended for use in contact with metals, because they are less reactive. Some studies show that a corrosive behavior is detected in some cases. Table 2.2 summarizes the properties and the compatibility of different PCMs with common materials and their behavior.

Capric Acid

Browne *et al*. [62] showed that capric acid had aggressive corrosive behavior with different materials. The authors showed that copper and brass were affected by pitting corrosion, but the corrosion rate was higher in the case of copper than brass. Aluminum was also affected by pitting corrosion after 540 days and the corrosion got progressively worse with a mass loss of 6% at the end of the test. Mild steel was adversely affected by this PCM, however no deep pitting was detected. In the case of stainless steel and Perspex, no sign of corrosion was detected, and the results of the corrosion tests were negligible.

Capric Acid (73.5%) + Myristic Acid (26.5%)

Ferrer *et al*. [53] detected that copper underwent corrosion and the solution became blue. In the case of carbon steel, a high extent of

corrosion was observed in the first week which may be explained by the passivation of the sample. No corrosion was detected at four and twelve weeks. Stainless steel 304, 316 and aluminum exhibited relatively low corrosion rate, under 1 mg/cm^{2}yr.

Table 2.2 Summary of corrosion effects using organic PCMs

PCM	Melting point (°C)	Heat fusion (kJ/kg)	Recommendations					Ref.
			Copper	Brass	Aluminum	Stainless Steel	Carbon Steel	
Capric acid	27.5-32.7	167	Caution	Caution	Caution	Use	Caution	62
Capric acid (73.5%) + myristic acid (26.5%)	21.4	152	Caution	---	Use	Use	Use	53
Capric acid (75.2%) + palmitic acid (24.8%)	17.7-22.8	153	Caution	Caution	Caution	Use	Caution	53,62
Capric acid (75.2%) + Lauric acid (24.8%)	18.9-22.3	116	Caution	Caution	Caution	Use	Caution	62
Lauric acid	42.6	211.6	Caution	---	Use	Use	Use	63
Myristic acid	53.8	192.0	Caution	---	Use	Use	Caution	63
Stearic Acid	53.8	174.6	Caution	---	Use	Use	Use	63
Palmitic acid	59.8	197.9	Caution	---	Use	Use	Caution	63
Glutaric acid			Caution	---	Caution	Use	---	64

Capric Acid (75.2%) + Palmitic Acid (24.8%)

Ferrer *et al*. [53] studied the behavior of this eutectic fatty acid PCM

in contact with common materials. The authors detected that the only material that experienced a remarkable weight loss during the 12 weeks of test was copper. Materials such as carbon steel exhibited passivation at the beginning due to the mass loss at the first week and subsequent constant value.

Lauric Acid

The behavior of lauric acid with common materials was tested under 910 thermal cycles by Sari and Kaygusuz [63]. The authors observed that stainless steel (SS 304 L), carbon steel (C 20) and aluminum did not exhibit any sign of corrosion on the surface, however, copper was slightly corroded. In terms of corrosion values, copper had the maximum values with a 15.232 mg/cm^2 of mass loss and $1.7 \cdot 10^2$ mg/day corrosion rate.

Myristic Acid

Myristic acid also had a corrosive behavior under 910 thermal cycles. Slight corrosion on the surface of carbon steel (C20) and copper was detected, with corrosion values (mass loss and corrosion rate) of 44.620 mg/cm^2 and $4.9 \cdot 10^2$ mg/day in the case of carbon steel and 15.437 mg/cm^2 and $1.6 \cdot 10^2$ mg/day with the copper. In contrast, stainless steel (SS 304 L) and aluminum did not show any sign of corrosion and the corrosion values were observed to be negligible for these materials [63].

Stearic Acid

Sari and Kaygusuz [63] observed that stainless steel (SS 304 L), carbon steel (C 20) and aluminum did not have any sign of corrosion on the surface, however, copper was mildly corroded with corrosion values (mass loss and corrosion rate) of 31.416 mg/cm^2 and $3.4 \cdot 10^2$ mg/day, under 910 thermal cycles.

Palmitic Acid

Stainless steel and aluminum were found to be corrosion resistant in contact with palmitic acid under 910 thermal cycles with low corrosion values. In contrast, copper and carbon steel (C20) were found to have slight corrosion on the surface [63].

Glutaric Acid

Raam Dheep and Sreekumar [64] observed that aluminum in contact with glutaric acid had a total mass loss of 11.2% with a corrosion rate of 10.9869 mg/cm^{2}yr. Also, pits on the aluminum surface were observed. In the case of copper, the total mass loss was 6.5% with a corrosion rate of 0.9423 mg/cm^{2}yr and the solution became green after sixty thermal cycles which occurred due to oxidation of the sample. Large pits were detected on the surface in this case. Stainless steel had better results with a mass loss of 1.41% and corrosion rate of 0.3004 mg/cm^{2}yr, but small pits were detected due to the rupture of the passive layer.

2.5 Conclusion

Solar energy has a wide variety of applications in both domestic and industrial use. This energy allows us to obtain, directly and without GHG emissions, heat and electricity at a cost that is currently competitive with other more polluting technologies. However, the availability of this energy is limited to daylight hours, thus, requiring efficient thermal storage systems.

The use of PCMs in solar energy technologies has allowed the option of storing thermal energy produced by the solar collectors during the day so that it is possible to have energy available during the night.

In addition, the use of PCMs in PV energy also allows increasing the efficiency of the PV modules by increasing the electricity generation. An innovative design of PV energy is hybrid solar energy (PV/T), where the overall panel efficiency is increased thanks to the use of the thermal energy generated in the PV module. The PCM volume provides a built-in heat accumulation system inside the PV/T module, saving space and simplifying the final installation. The choice of PCM used in each solar energy application must be made considering both the thermophysical properties of the PCM and the compatibility between the different materials of the system, as has been outlined in this chapter.

Acknowledgements

David González Peña thank Junta de Castilla-León for economic support (PIRTU Program, ORDEN EDU/310/2015).

References

1. Atkin, P., and Farid, M. M. (2015) Improving the efficiency of photovoltaic cells using PCM infused graphite and aluminium fins. *Solar Energy*, **114**, 217-228.
2. Evans, A., Strezov, V., and Evans, T. J. (2009) Assessment of sustainability indicators for renewable energy technologies. *Renewable and Sustainable Energy Reviews*, **13**(5), 1082-1088.
3. Renewable Power Generation Costs in 2017, *IRENA* (2018). Online: https://www.irena.org/publications/2018/Jan/Renewable-power-generation-costs-in-2017 [accessed 19th December 2018].
4. Biyik, E., Araz, M., Hepbasli, A., Shahrestani, M., Yao, R., Shao, L., Essah, E., Oliviera, A. C., del Cano, T., Rico, E., Lechon, J. L., Andrade, L., Mendes, A., and Atli, Y. B. (2017) A key review of building integrated photovoltaic (BIPV) systems. *Engineering Science and Technology, an International Journal*, **20**(3), 833-858.
5. Oliver, M., and Jackson, T. (2001) Energy and economic evaluation of building-integrated photovoltaics. *Energy*, **26**(4), 431-439.
6. Collares-Pereira. M., Goodman, N. B., Greenman, P., O'Gallagher, J., Rabl, A., Simmons, H., Wharton, L., and Winston, R. (1978) Compound parabolic concentrators with non-evacuated receivers - Prototype performance and a larger scale demonstration in a school heating system. *Sun: Mankind's Future Source Energy*, **2**, 1227-1232.
7. Zacharopoulos, A., Eames, P. C., McLarnon, D., and Norton, B. (2000) Linear dielectric non-imaging concentrating covers for PV integrated building facades. *Solar Energy*, **68**, 439-452.
8. Stropnik, R., and Stritih, U. (2016) Increasing the efficiency of PV panel with the use of PCM. *Renewable Energy*, **97**, 671-679.
9. Hasan, A., McCormack, S. J., Huang, M. J., and Norton, B. (2010) Evaluation of phase change materials for thermal regulation enhancement of building integrated photovoltaics. *Solar Energy*, **84**, 1601-1612.
10. Browne, M. C., Norton, B., and McCormack, S. J. (2016) Heat retention of a photovoltaic/thermal collector with PCM. *Solar Energy*, **133**, 533-548.
11. Ames, W. (1983) Photovoltaic Devices for Producing Electrical and Heat Energy, patent US 4389533.
12. Pal, D., and Joshi, Y. K. (1999) Thermal Control of Horizontally Mounted Heat Sources using Phase Change Materials. *Proceedings of InterPACk'99*, volume 2, pp. 1625-1630.
13. Griffiths, P. W., and Eames, P. C. (2007) Performance of chilled ceiling panels using phase change material slurries as the heat transport medium. *Applied Thermal Engineering*, **27**(10), 1756-1760.
14. Browne, M. C., Norton, B., and McCormack, S. J. (2015) Phase change

materials for photovoltaic thermal management. *Renewable and Sustainable Energy Reviews*, **47**(244), 762-782.
15. Gunther, E., Hiebler, S., Mehling, H., and Redlich, R. (2009) Enthalpy of phase change materials as a function of temperature: Required accuracy and suitable measurement methods. *International Journal of Thermophysics*, **30**(4), 1257-1269.
16. Cabeza, L. F., Castell, A., Barreneche, C., De Gracia, A., and Fernández, A. I. (2011) Materials used as PCM in thermal energy storage in buildings: A review. *Renewable and Sustainable Energy Reviews*, **15**(3), 1675-1695.
17. Pereira da Cunha, J., and Eames, P. (2016) Thermal energy storage for low and medium temperature applications using phase change materials - A review. *Applied Energy*, **177**, 227-238.
18. Xu, B., Li, P., and Chan, C. (2015) Application of phase change materials for thermal energy storage in concentrated solar thermal power plants: A review to recent developments. *Applied Energy*, **160**, 286-307.
19. Siegel, R. (1977) Solidification of low conductivity material containing dispersed high conductivity particles. *International Journal of Heat and Mass Transfer*, **20**(10), 1087-1089.
20. Cabeza, L. F., Mehling, H., Hiebler, S., and Ziegler, F. (2002) Heat transfer enhancement in water when used as PCM in thermal energy storage. *Applied Thermal Engineering*, **22**(10), 1141-1151.
21. Huang, M. J., Eames, P. C., and Norton, B. (2004) Thermal regulation of building-integrated photovoltaics using phase change materials. *International Journal of Heat and Mass Transfe*r, **47**(12-13), 2715-2733.
22. Huang, M. J. Eames, P. C., and Hewitt, N. J. (2006) The application of a validated numerical model to predict the energy conservation potential of using phase change materials in the fabric of a building. *Solar Energy Materials and Solar Cells*, **90**(13), 1951-1960.
23. Hasan, A., McCormack, S., Huang, M., and Norton, B. (2014) Energy and cost saving of a photovoltaic-phase change materials (PV-PCM) system through temperature regulation and performance enhancement of photovoltaics. *Energies*, **7**(3), 1318-1331.
24. Huang, M. J., Eames, P. C., and Norton, B. (2006) Phase change materials for limiting temperature rise in building integrated photovoltaics. *Solar Energy*, **80**(9), 1121-1130.
25. Browne, M. C., Lawlor, K., Kelly, A., Norton, B., and Cormack, S. J. (2015) Indoor characterisation of a photovoltaic/thermal phase change material system. *Energy Procedia*, **70**, 163-171.
26. Huang, M. J., Eames, P. C., Norton, B., and Hewitt, N. J. (2011) Natural convection in an internally finned phase change material heat sink for the thermal management of photovoltaics. *Solar Energy Materials and Solar Cells*, **95**(7), 1598-1603.

27. Guney, M. S. (2016) Solar power and application methods. *Renewable and Sustainable Energy Reviews*, **57**, 776-785.
28. Mekhilef, S., Saidur, R., and Safari, A. (2011) A review on solar energy use in industries. *Renewable and Sustainable Energy Reviews*, **15**(4), 1777-1790.
29. Kalogirou, S. A. (2004) Solar thermal collectors and applications. *Progress in Energy and Combustion Science*, **30**(3), 231-295.
30. Sharif, M. K. A., Al-Abidi, A. A., Mat, S., Sopian, K., Ruslan, M. H., Sulaiman, M. Y., and Rosli, M. A. M. (2015) Review of the application of phase change material for heating and domestic hot water systems. *Renewable and Sustainable Energy Reviews*, **42**, 557-568.
31. Kenisarin, M., and Mahkamov, K. (2007) Solar energy storage using phase change materials. *Renewable and Sustainable Energy Reviews*, **11**(9), 1913-1965.
32. Mazman, M., Cabeza, L. F., Mehling, H., Nogues, M., Evliya, H., and Paksoy, H. O. (2009) Utilization of phase change materials in solar domestic hot water systems. *Renewable Energy*, **34**(6), 1639-1643.
33. Padovan, R., and Manzan, M. (2014) Genetic optimization of a PCM enhanced storage tank for solar domestic hot water systems. *Solar Energy*, **103**, 563-573.
34. Nallusamy, N., Sampath, S., and Velraj, R. (2007) Experimental investigation on a combined sensible and latent heat storage system integrated with constant/varying (solar) heat sources. *Renewable Energy*, **32**(7), 1206-1227.
35. Ibanez, M., Cabeza, L. F., Sole, C., Roca, J., and Nogues, M. (2006) Modelization of a water tank including a PCM module. *Applied Thermal Engineering*, **26**(11-12), 1328-1333.
36. Wang, Z. Qiu, F. Yang, W. and Zhao, X. (2015) Applications of solar water heating system with phase change material. *Renewable and Sustainable Energy Reviews*, **52**, 645-652.
37. Tian, Y., and Zhao, C. Y. (2013) A review of solar collectors and thermal energy storage in solar thermal applications. *Applied Energy*, **104**, 538-553.
38. *Concentrating Solar Power Projects*, NREL, USA. Online: https://solarpaces.nrel.gov [accessed 17th December 2018].
39. Alva, G., Liu, L., Huang, X., and Fang, G. (2017) Thermal energy storage materials and systems for solar energy applications. *Renewable and Sustainable Energy Reviews*, **68**, 693-706.
40. Bauer, T., Pfleger, N., Laing, D., Steinmann, W. D., Eck, M., and Kaesche, S. (2013) High-temperature molten salts for solar power application. In: *Molten Salts Chemistry*, Lantelme, F., and Groult, H. (eds.), Elsevierm, USA, pp. 415-438.
41. Nomura, T., Okinaka, N., and Akiyama, T. (2010) Technology of latent heat storage for high temperature application: A review. *ISIJ International*, **50**(9), 1229-1239.

42. Sarvghad, M., Maher, S. D., Collard, D., Tassan, M., Will, G., and Steinberg, T. A. (2018) Materials compatibility for the next generation of concentrated solar power plants. *Energy Storage Material*, **14**, 179-198.
43. Ma, T., Yang, H., Zhang, Y., Lu, L., and Wang, X. (2015) Using phase change materials in photovoltaic systems for thermal regulation and electrical efficiency improvement: A review and outlook. *Renewable and Sustainable Energy Reviews*, **43**, 1273-1284.
44. Ling, Z. Zhang, Z. Shi, G., Fang, X., Wang, L., Gao, X., Fang, Y., Xu, T., Wang, S., and Liu X. (2014) Review on thermal management systems using phase change materials for electronic components, Li-ion batteries and photovoltaic modules. *Renewable and Sustainable Energy Reviews*, **31**, 427-438.
45. Radziemska, E. (2003) The effect of temperature on the power drop in crystalline silicon solar cells. *Renewable Energy*, **28**(1), 1-12.
46. Browne M. C., Quigley, D., Hard, H. R., Gilligan, S., Ribeiro, N. C. C., Almeida, N., and McCormack, S. J. (2016) Assessing the thermal performance of phase change material in a photovoltaic/thermal system. *Energy Procedia*, **91**, 113-121.
47. Makki, A., Omer, S., and Sabir, H. (2015) Advancements in hybrid photovoltaic systems for enhanced solar cells performance. *Renewable and Sustainable Energy Reviews*, **41**, 658-684.
48. Al-Waeli, A. H. A., Sopian, K., Kazem, H. A., and Chaichan, M. T. (2017) Photovoltaic/Thermal (PV/T) systems: Status and future prospects. *Renewable and Sustainable Energy Reviews*, **77**, 109-130.
49. Yin, H. M., Yang, D. J., Kelly, G., and Garant, J. (2013) Design and performance of a novel building integrated PV/thermal system for energy efficiency of buildings. *Solar Energy*, **87**, 84-195.
50. Malvi, C. S., Dixon-Hardy, D. W., and Crook, R. (2011) Energy balance model of combined photovoltaic solar-thermal system incorporating phase change material. *Solar Energy*, **85**(7), 1440-1446.
51. *Hybrid*, Solimpeks Solar Corp. (2016). Online: http://www.solimpeks.com/tax-product/hybrid/ [accessed 07th January 2019].
52. Moreno, P., Miro, L., Sole, A., Barreneche, C., Sole, C., Martorell, I., and Cabeza, L. F. (2014) Corrosion of metal and metal alloy containers in contact with phase change materials (PCM) for potential heating and cooling applications. *Applied Energy*, **125**, 238-245.
53. Ferrer, G., Sole, A., Barreneche, C., Martorell, I., and Cabeza, L. F. (2015) Corrosion of metal containers for use in PCM energy storage. *Renewable Energy*, **76**, 465-469.
54. Cabeza, L. F., Illa, J., Roca, J., Badia, F., Mehling, H., Hiebler, S., and Ziegler, F. (2001) Middle term immersion corrosion tests on metalsalt hydrate pairs used for latent heat storage in the 32 to 36 °C temperature range. *Materials and Corrosion*, **52**(10), 748-754.
55. Taylor, M. M., Cabeza, L. F., Marmer, W. N., and Brown, E. M. (2001)

Enzymatic modification of hydrolysis products from collagen using a microbial transglutaminase. I. Physical properties. *Journal of American Leather Chemists Association*, **96**(9), 319-332.

56. Cabeza, L. F., Roca, J., As, M. N., Mehling, H., and Hiebler, S. (2002) Immersion corrosion tests on metal-salt hydrate pairs used for latent heat storage in the 48 to 58°C temperature range. *Materials and Corrosions*, **53**, 902-907.
57. Garcia-Romero, A., Delgado, A., Urresti, A., Martin, K., and Sala, J. M. (2009) Corrosion behaviour of several aluminium alloys in contact with a thermal storage phase change material based on Glauber's salt. *Corrosion Science*, **51**(6), 1263-1272.
58. Danielik, V., Soska, P., and Felgerova, K. (2016) Corrosive effects of nitrate-containing phase change materials used with copper. *Acta Chimica Slovaca*, **9**(2), 75-83.
59. Danielik, V., Soska, P., Felgerovi, K., and Zemanovi, M. (2017) The corrosion of carbon steel in nitrate hydrates used as phase change materials. *Materials and Corrosions*, **68**(4), 416-422.
60. Gutierrez, A., Ushaka, S., Mamania, V., Vargas, P., Barreneche, C., Cabeza, L. F., and Grageda M. (2017) Characterization of wastes based on inorganic double salt hydrates as potential thermal energy storage materials. *Solar Energy Materials and Solar Cells*, **170**, 149-159.
61. Ren, S. J., Charles, J., Wang, X. C., Nie, F. X., Romero, C., Neti, S., Zheng, Y., Hoenig, S., Chen C., Cao F., Bonner, R., and Pearlman, H. (2017) Corrosion testing of metals in contact with calcium chloride hexahydrate used for thermal energy storage. *Materials and Corrosion*, **68**(10), 1046-1056.
62. Browne, M. C., Boyd, E., and Mccormack, S. J. (2017) Investigation of the corrosive properties of phase change materials in contact with metals and plastic. *Renewable Energy*, **108**, 555-568.
63. Sari, A., and Kaygusuz, K. (2003) Some fatty acid used for latent heat storage: thermal stability and corrosion of metals with respect to thermal cycling. *Renewable Energy*, **28**, 939-948.
64. Raam Dheep G., and Sreekumar, A. (2018) Investigation on thermal reliability and corrosion characteristics of glutaric acid as an organic phase change material for solar thermal energy storage applications. *Applied Thermal Engineering*, **129**, 1189-1196.